# Monte Carlo Simulation of Electric Vehicle Charging Schemes for an EV Aggregator Offering Ancillary Services Under Grid Limitations

Dita Anggraini*, Mikael Amelin, and Lennart Söder
*Division of Electric Power and Energy Systems*
*KTH Royal Institute of Technology*
Stockholm, Sweden
Email: *ditaa@kth.se

***Abstract*—The growing adoption of electric vehicles (EVs) presents challenges for power systems, particularly due to uncontrolled charging. Such charging can lead to grid overload that requires immediate grid reinforcement. This paper proposes a planning model for an EV aggregator participating in ancillary service markets while considering the distribution grid limitations. Monte Carlo simulations capture uncertainties in mobility patterns and activations of the ancillary services. We compare uncontrolled charging with a bidirectional smart charging algorithm, which is formulated as a mixed-integer linear program. A case study focusing on the Swedish market, specifically regarding participation in the frequency containment reserve, demonstrates that smart charging benefits the EV aggregator, EV owners, and the power system. The results highlight that the flexibility of the EV can optimize the existing utilization of the grid and delay the reinforcement of the grid. The proposed planning model supports decision-making in uncertain markets, ensuring the feasibility of the EV aggregator business model.**

***Index Terms*—Ancillary Services, Electric Vehicle Aggregators, Grid Limitations, Mixed-Integer Linear Programming, Monte Carlo Simulations.**

## I. Introduction

The growing penetration of Electric Vehicles (EVs) presents challenges and opportunities for power systems. Aggregated uncontrolled EV charging can significantly impact grid stability as EV adoption grows, especially regarding voltage deviations, distribution transformer load, and higher power losses [1]. EV aggregators can address these issues by managing and coordinating EV charging and discharging schedules [2]. They act as intermediaries between EV owners and the electricity market actors [3], send bids to the ancillary service markets and control the charging/discharging power signals. To ensure efficient market integration, the interactions between EV aggregators and other electricity market participants require further investigation.

A primary challenge in the EV aggregator planning model includes uncertainties in mobility patterns, electricity prices, ancillary service activations, and grid conditions. Ref [4] proposed a planning model for an investor offering ancillary services using EVs or energy storage systems (ESSs) to maximize long-term payoffs. The study finds that investing in EVs is more profitable due to high ESS initial investment costs. The study has not considered grid conditions in its algorithm. While [5] presents an EV scheduling algorithm that considers the triple-level benefits of EV owners, aggregators, and distribution grid, it does not address the stochastic uncertainties and grid limitations in the model. The gaps in the previous research underscore the need for further research incorporating both the stochastic nature of EV charging and grid limitations.

This paper proposes an EV aggregator's planning model that explicitly accounts for the uncertainties of EV charging, ancillary service activations, and physical distribution grid limitations. The models will be simulated as Monte Carlo simulations. Uncontrolled EV charging will be used as the baseline model. A bidirectional smart charging, often called Vehicle to Grid (V2G) will be modeled in the proposed EV aggregator planning model. In the V2G concept, EVs that are connected to the grid can draw and supply a controlled amount of electricity from/to the grid [6]. The rest of the paper is structured as follows: section II provides relevant information about Swedish ancillary service markets, section III explains the mathematical formulation of the proposed planning model, section IV discusses the case study, section V analyzes the simulation results, and section VI concludes the discussions and introduces the future work.

## II. Swedish Ancillary Service Markets

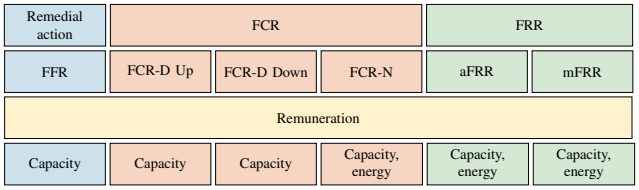


Fig. 1. Swedish ancillary service markets [7]

Ancillary services support the reliability and stability of the power system in Sweden; these services are managed by Svenska Kräfnat (SvK); the summary of the services is given in Fig. 1. Historically, Frequency Containment Reserve (FCR) offered higher revenue potential than other ancillary services [8]. Therefore, in this study, we will focus on FCR.

979-8-3315-1278-1/25/$31.00 ©2025 IEEE

FCR consists of FCR-Normal (FCR-N) and FCR-Disturbance (FCR-D). Both have capacity markets where actors can offer bids and supply the services. The minimum bid size for FCR is 0.1 MW [9]. The accepted bid capacities must be available during the delivery periods, even though not all bids need to be activated. A more detailed overview of other ancillary service types is available in the Appendix A.

FCR-N handles the frequency deviation between 49.9–50.1 Hz. It is a symmetrical product that applies to up and down-regulation. The endurance needed is 1 hour at 100% activation. Compensations are given for both capacity and energy activation. Capacity remuneration is symmetric for up-and down-regulation, while energy remuneration is given according to the prices of up- or down-regulation [9].

The FCR-D is designed to handle more severe frequency deviation. This product is not symmetrical and has two markets for FCR-D up and down regulations. FCR-D up and down regulations handle frequency deviation between 49.90–49.50 Hz and 50.10–50.50 Hz, respectively [10]. There is only a capacity remuneration for FCR-D products; the endurance of the service is 20 minutes [9].

## III. Mathematical Formulation

Two models were developed in this study. The first is an uncontrolled charging model, which is the baseline case. The latter is the bidirectional charging planning model, which is the proposed planning model for the EV aggregator. Unidirectional smart charging is intentionally excluded in this study since the primary objective is to evaluate the techno-economic potential of V2G technology. While unidirectional charging is effective for managing load and optimizing charging costs, it does not offer the additional benefits associated with grid services that bidirectional smart charging can provide. A brief discussion about Monte Carlo simulations is available in Appendix B. Meanwhile, the roles of the key stakeholders within the model are defined as follows:

- **Aggregator**: it controls the charging/discharging signals of the EVs and sells ancillary services in FCR market.
- **EV owners**: they have take-and-pay contracts with variable prices (spot prices), and charging preferences, represented by their arrival time, departure time, desired and maximum State of Charge (SoC).
- **Grid owner**: set grid limitations in the model.
- **Retailer**: it sells energy to the EV owners and forecasts load for trading in the spot market.

Based on the defined stakeholder's roles above, the two charging models are formulated as follows:

### A. Uncontrolled Charging

In uncontrolled charging, EVs are charged immediately upon being plugged in. EVs are plugged instantaneously after their arrival time ($t_i^{\text{arr}}$), disregarding other factors such as charging prices ($\lambda_t^{\text{Chg}}$), grid capacity, or optimal charging time. EV batteries are charged with maximum output power ($\bar{P}_i^{\text{EV,max}}$) after $t_{\text{arr}}^i$ until the batteries reach the desired SoC ($SoC_i^{\text{Des}}$) or departure time ($t_{\text{dep}}^i$), whatever occurs first. The charging power ($P_{i,t}^{\text{Chg}}$) for uncontrolled charging is given as follows:

$$P_{i,t}^{\text{Chg}} = \begin{cases} \bar{P}_i^{\text{EV,max}}, & \text{if } E_{i,t-1} + \eta_i^{\text{Chg}} \bar{P}_i^{\text{EV,max}} \Delta t \leq \overline{SoC}_i \overline{E}_i, \\ \frac{\overline{SoC}_i \overline{E}_i - E_{i,t-1}}{\Delta t}, & \text{if } E_{i,t-1} + \eta_i^{\text{Chg}} \bar{P}_i^{\text{EV,max}} \Delta t > \overline{SoC}_i \overline{E}_i \ \& \ E_{i,t-1} < \overline{SoC}_i \overline{E}_i, \\ 0, & \text{if } E_{t-1}^i = \overline{SoC}_i \overline{E}_i. \end{cases} \tag{1}$$

$\overline{SoC}_i$, $\overline{E}_i$, and $\eta_i^{\text{Chg}}$ are the maximum allowed SoC, maximum battery capacity, and charging efficiency of EV $i$. $\Delta t$ is the simulation time step and $E_{i,t}$ is the battery capacity at time $t$. For EV $i$, SoC at time $t$ ($SOC_{i,t}$) can be computed below:

$$SOC_{i,t} = SOC_{i,t-1} + \frac{\left(\eta_i^{\text{Chg}} P_{i,t}^{\text{Chg}} \Delta t\right)}{\overline{E}_i}. \tag{2}$$

The SoC in the arrival time ($SoC_{i,t_{\text{arr}}}$) is randomized as a uniform distribution. Since the charging power affects the EV battery degradation, it must be considered in the costs. The average battery degradation cost ($\delta_i^{\text{Deg}}$) is given as:

$$\delta_i^{\text{Deg}} = \frac{C_i^{\text{Inv}}}{2 L_i \overline{E}_i DoD_i}. \tag{3}$$

$C_i^{\text{Inv}}$, $L_i$ and $DoD_i$ are battery investment costs, number of full cycles before the End of Life (EoL), and maximum Depth of Discharge (DoD) that can be handled by EV $i$. While a more detailed battery degradation model incorporating relevant factors such as DoD and reduced charging capability during higher SoC can enhance the accuracy of the cost computation, it significantly increases the model complexity and computation time. The simplified battery degradation cost model in (3) is intentionally chosen for practical feasibility and stability of the EV scheduling model later on. The total charging costs of EV $i$ paid by the EV owners ($C^{\text{tot,Unc}}$] can be computed as:

$$C^{\text{tot,Unc}} = \sum_{i=1}^{I} \sum_{t=1}^{T} \left(\lambda_t^{\text{Chg}} + \delta_i^{\text{Deg}}\right) P_{i,t}^{\text{Chg}} \Delta t. \tag{4}$$

$I$ and $T$ denote the number of EVs and maximum time step in the planning model, respectively.

### B. Bidirectional Smart Charging (V2G)

In the V2G model, the EV aggregator controls the charging/discharging schedules for the EVs within the contracted area. In this study, the objective of the optimization problem is to maximize the revenue of the EV aggregators.

$$C_{i,t}^{\text{FCR}_{\text{N,cap}}} = \alpha_{i,t}^{\text{FCR}_{\text{N}}} \lambda_t^{\text{FCR}_{\text{N,cap}}} P_{i,t}^{\text{FCR}_{\text{N}}}, \tag{5a}$$

$$C_{i,t}^{\text{FCR}_{\text{N,ene}}^{\text{U/D}}} = \alpha_{i,t}^{\text{FCR}_{\text{N}}} \lambda_t^{\text{FCR}_{\text{N}}^{\text{U/D,ene}}} \gamma_{i,t}^{\text{FCR}_{\text{N}}^{\text{U/D}}} P_{i,t}^{\text{FCR}_{\text{N}}} \Delta t, \tag{5b}$$

$$C_{i,t}^{\text{FCR}_{\text{D,cap}}^{\text{U/D}}} = \alpha_{i,t}^{\text{FCR}_{\text{D}}^{\text{U/D}}} \lambda_t^{\text{FCR}_{\text{D}}^{\text{U/D,cap}}} P_{i,t}^{\text{FCR}_{\text{D}}^{\text{U/D}}}, \tag{5c}$$

$$C_{i,t}^{\text{Dis}} = \lambda_t^{\text{Dis}} P_{i,t}^{\text{Dis}} \Delta t, \tag{5d}$$

$$C_{i,t}^{\text{Deg}} = \delta_i^{\text{Deg}} (x_{i,t}^{\text{Chg}} P_{i,t}^{\text{Chg}} + x_{i,t}^{\text{Dis}} P_{i,t}^{\text{Dis}}) \Delta t. \tag{5e}$$

It is assumed that the EV aggregators only participate in the FCR market through bidirectional smart charging, with all the

necessary technologies available to support the operation. The optimization model's objective is to maximize EV aggregators' revenue. The revenues and costs of the EV aggregators come from different sources. These costs can be computed such as in (5). $C_{i,t}^{\mathrm{FCR_{N,cap}}}$, $C_{i,t}^{\mathrm{FCR_{N,ene}^{U/D}}}$, $C_{i,t}^{\mathrm{FCR_{D,cap}^{U/D}}}$, $C_{i,t}^{\mathrm{Dis}}$, and $C_{i,t}^{\mathrm{Deg}}$ denote the FCR-N reserve capacity remuneration, FCR-N up/down energy activation remuneration, FCR-D up/down-regulation capacity remuneration, costs to pay EV owners when discharging their batteries, and compensation for the battery degradation. The V2G optimization problem is formulated as follows:

$$\max \sum_{i=1}^{I}\sum_{t=1}^{T}\Big(C_{i,t}^{\mathrm{FCR_{N,cap}}} + C_{i,t}^{\mathrm{FCR_{N,ene}^{U}}} + C_{i,t}^{\mathrm{FCR_{N,ene}^{D}}} + C_{i,t}^{\mathrm{FCR_{D,cap}^{U}}} + C_{i,t}^{\mathrm{FCR_{D,cap}^{D}}} - C_{i,t}^{\mathrm{Dis}} - C_{i,t}^{\mathrm{Deg}}\Big), \tag{6a}$$

s.t:

$$\frac{P_{i,t}^{\mathrm{Chg}}}{\eta_i^{\mathrm{Chg}}} - P_{i,t}^{\mathrm{Dis}}\eta_i^{\mathrm{Dis}} + \gamma_{i,t}^{\mathrm{FCR_N^U}}P_{i,t}^{\mathrm{FCR_N}} - \gamma_{i,t}^{\mathrm{FCR_N^D}}P_{i,t}^{\mathrm{FCR_N}} + \alpha_{i,t}^{\mathrm{FCR_D^U}}P_{i,t}^{\mathrm{FCR_D^U}} - \alpha_{i,t}^{\mathrm{FCR_D^D}}P_{i,t}^{\mathrm{FCR_D^D}} \geq 0, \tag{6b}$$

$$P_{i,t}^{\mathrm{Chg}} = \gamma_{i,t}^{\mathrm{FCR_D^D}}P_{i,t}^{\mathrm{FCR_D^D}} + \gamma_{i,t}^{\mathrm{FCR_N^D}}P_{i,t}^{\mathrm{FCR_N}}, \tag{6c}$$

$$P_{i,t}^{\mathrm{Dis}} = \gamma_{i,t}^{\mathrm{FCR_D^U}}P_{i,t}^{\mathrm{FCR_D^U}} + \gamma_{i,t}^{\mathrm{FCR_N^U}}P_{i,t}^{\mathrm{FCR_N}}, \tag{6d}$$

$$SoC_{i,t+1} = SoC_{i,t} + \left(\eta_i^{\mathrm{Chg}}\, x_{i,t}^{\mathrm{Chg}}\, P_{i,t}^{\mathrm{Chg}}\Delta t\right)/\bar{E}_i - \left(x_{i,t}^{\mathrm{Dis}}\, P_{i,t}^{\mathrm{Dis}}\Delta t\right)/\left(\eta_i^{\mathrm{Dis}}\bar{E}_i\right), \tag{6e}$$

$$P_{i,t}^{\mathrm{FCR_D^U}} + P_{i,t}^{\mathrm{FCR_D^D}} + P_{i,t}^{\mathrm{FCR_N}} \leq \frac{SoC_{i,t}\,\bar{E}_i}{\eta_i^{\mathrm{Dis}}}, \tag{6f}$$

$$D_t^{\mathrm{Tot}} + \sum_{i=1}^{I}\left(\frac{x_{i,t}^{\mathrm{Chg}}\, P_{i,t}^{\mathrm{Chg}}}{\eta_i^{\mathrm{Chg}}} - x_{i,t}^{\mathrm{Dis}}\, P_{i,t}^{\mathrm{Dis}}\eta_i^{\mathrm{Dis}}\right) \leq \overline{P^{\mathrm{Tot}}}, \tag{6g}$$

$$D_{i,t} + \left(\frac{x_{i,t}^{\mathrm{Chg}}\, P_{i,t}^{\mathrm{Chg}}}{\eta_i^{\mathrm{Chg}}} - x_{i,t}^{\mathrm{Dis}}\, P_{i,t}^{\mathrm{Dis}}\eta_i^{\mathrm{Dis}}\right) \leq P_i^{\mathrm{Sub}}, \tag{6h}$$

$$\underline{SoC}_i \leq SoC_{i,t} \leq \overline{SoC}_i, \tag{6i}$$

$$SoC_i^{\mathrm{Des}} \leq SoC_{i,t_{\mathrm{dep}}} \leq \overline{SoC}_i, \tag{6j}$$

$$\alpha_{i,t}^{\mathrm{FCR_D^U}} + \alpha_{i,t}^{\mathrm{FCR_D^D}} \leq 1, \tag{6k}$$

$$x_{i,t}^{\mathrm{Chg}} + x_{i,t}^{\mathrm{Dis}} \leq 1, \tag{6l}$$

$$0 \leq \gamma_{i,t}^{\mathrm{FCR_N^U}},\ \gamma_{i,t}^{\mathrm{FCR_N^D}} \leq 1, \tag{6m}$$

$$0 \leq \gamma_{i,t}^{\mathrm{FCR_D^U}},\ \gamma_{i,t}^{\mathrm{FCR_D^D}} \leq 1, \tag{6n}$$

$$0 \leq P_{i,t}^{\mathrm{Chg/Dis}} \leq \overline{P_i^{\mathrm{Chg/Dis}}}, \tag{6o}$$

$$0 \leq P_{i,t}^{\mathrm{FCR_D^{U/D}}} \leq \alpha_{i,t}^{\mathrm{FCR_D^{U/D}}} \cdot \bar{P}_i^{\mathrm{EV,max}}, \tag{6p}$$

$$0 \leq P_{i,t}^{\mathrm{FCR_N}} \leq \alpha_{i,t}^{\mathrm{FCR_N}} \cdot \bar{P}_i^{\mathrm{EV,max}}, \tag{6q}$$

$$\alpha_{i,t}^{\mathrm{FCR_N}},\ \alpha_{i,t}^{\mathrm{FCR_D^U}},\ \alpha_{i,t}^{\mathrm{FCR_D^D}} \in \{0,1\}, \tag{6r}$$

$$\forall\, t = 1,\ldots,T, \quad \forall\, i = 1,\ldots,I. \tag{6s}$$

$\lambda_t^{\mathrm{FCR_{N,cap}}}$, $\lambda_t^{\mathrm{FCR_N^{U/D,ene}}}$, $\lambda_t^{\mathrm{FCR_D^{U/D,cap}}}$, and $\lambda_t^{\mathrm{Dis}}$, are the prices for FCR-N capacity, FCR-N up/down regulation energy, FCR-D up/down capacity, and discharging compensation for EV owners. $\alpha_{i,t}^{\mathrm{FCR_N}}$ and $\alpha_{i,t}^{\mathrm{FCR_D^{U/D}}}$ are the binary decision variables for bid acceptance for FCR-N and FCR-D up/down, the value is 1 if it the bid is accepted and 0 if not. Not all accepted capacities are activated, $\gamma_{i,t}^{\mathrm{FCR_N^{U/D}}}$ and $\gamma_{i,t}^{\mathrm{FCR_D^{U/D}}}$ are continuous variables from 0 to 1 that represent the energy activation rates of FCR-N up/down and FCR-D up/down. $x_{i,t}^{\mathrm{Chg/Dis}}$ is the binary number for EV charging/discharging, 1 if it occurs and 0 if not, to avoid charging/discharging in an EV occurs simultaneously. $P_{i,t}^{\mathrm{FCR_N}}$, $P_{i,t}^{\mathrm{FCR_D^{U/D}}}$, and $P_{i,t}^{\mathrm{Dis}}$ are the power of the FCR-N capacity, FCR-D up/down capacity, and EV discharge. $\eta_i^{\mathrm{Dis}}$ is the discharge efficiency. In reality, charging/discharging efficiency depends on the SoC levels due to the changing internal resistance [11]. However, in this study, a constant charging/discharging efficiency is assumed to simplify the mathematical model. This simplification is required to maintain computational tractability without affecting the accuracy of the solution too much. $\underline{SoC}_i$, $SoC_i^{\mathrm{Des}}$, and $SoC_{i,t_{\mathrm{dep}}}$ are the minimum allowed SoC, desired SoC, and SoC at the departure time. $\overline{P^{\mathrm{Tot}}}$ and $P_i^{\mathrm{Sub}}$ are the subscribed power limit of the distribution transformer and individual house. $D_t^{\mathrm{Tot}}$ and $D_{i,t}$ are the aggregated base household load and individual house load, respectively.

The V2G optimization problem is given in (6). Equation (6a) is the objective function to maximize the EV aggregator's revenue. Equations (6b), (6c), (6d), (6e), and (6f) denote the power balance, charging power balance, discharging power balance, SoC balance, and maximum ancillary service power. The subscribed powers in the distribution feeder and individual house are limited by (6g) and (6h). Variable limits for SoC and SoC at the departure time are given in (6i) and (6j). Equation (6k) shows that the FCR-D up/down-regulation does not coincide. A similar constraint applies for charging/discharging power, given in (6l). Equations (6m) and (6n) are variable limits for the continuous energy activation variable. The maximum power for FCR services is set by (6o), (6p), (6q). The binary variable for the bid acceptance is set by (6r), and finally, (6s) applies to equations in (6).

## IV. Case Study

### A. Simulation Setup and Assumptions

Several simplifications have been incorporated into the simulations. In this model, the EV aggregator focuses solely on the FCR market, operating under the assumption of perfect information. Input data is derived from historical statistics, giving a foundation for the analysis. All the necessary technologies and infrastructures for V2G operations are also assumed to be readily available. The simulation is performed with a 15-minute time resolution, reflecting the Swedish market clearing.

The endurance for FCR-D activation is assumed to fall within each time step, while the activation rate for FCR-N is always the same for four consecutive time steps. Although there is a minimum bid requirement of 0.1 MW for the FCR in real-world scenarios, this constraint is excluded from the case study due to the size of the distribution network and the number of EVs involved in the model. Importantly, the

algorithm and simulations are scalable and can effectively be applied to larger systems. The EVs are assumed to be available and connected to the grid throughout their parking duration.

To participate in the V2G program, EV owners need to enter the information required by the EV aggregator to plan its operation; such information includes: battery types, charger specifications, minimum/maximum allowed SoC, desired SoC, and expected travel time. One thousand scenarios of Monte Carlo Simulations are performed. The simulations were performed on a Dell Inc. Latitude 7440 computer equipped with 13th Gen Intel(R) Core(TM) i7-1365U 1.80 GHz processor, 32 GB RAM, and a 64-bit operating system. The computations were implemented using Python 3.9.13 with Gurobi 11.0.2 solver for optimization and NumPy, Pandas, and Matplotlib for data processing and visualization.

### B. Distribution Test System

To test the algorithm, we use a modified IEEE European Low Voltage (LV) test feeder [12]. The network is a radial structure representing a suburban area with overhead lines. The network comprises 55 residential customers connected to a 230/400 V, 50 Hz system. The substation transformer is rated at 400 kVA, stepping down from 20 kV to 0.4 kV, and operates with a utilization rate of 0.95 and a power factor of 0.95. Each customer is protected by a 32 A fuse. For this simulation, all loads are assumed to be balanced and connected in a three-phase configuration. The single-line diagram of this modified system is attached in Appendix C, in Fig. 5. Furthermore, the IEEE LV test feeder load profile is scaled by a factor of 7.36 to match the typical annual energy consumption of a household in Sweden, which is approximately 23.83 MWh/year [13].

### C. Input Data

*1) Mobility Patterns:* Mobility data from the Swedish National Travel Survey [14] is used in the case study. The travel statistic is fitted with a suitable Probability Distribution Function (PDF). Both arrival and departure time PDFs can be modeled by bimodal distribution, while travel distance is modeled using the extreme value distribution. The PDFs are given in Fig. 6 and 7 in Appendix D.

*2) EV Specifications:* Four EV types used in [15] will be adopted to model different types of EVs. These are the four most popular EV types in Sweden, according to [16]. In summary, the four types have specifications, as shown in Table III. The overall charge/discharge efficiency cycle is typically 90-95%. The charging process is more efficient than discharging due to lower losses and higher charging voltage [17]. To model this, charging/discharging efficiencies are assumed to be 0.95/0.90 for all EV types. All types of EVs have 11 kW charging power. The SoC levels will be kept between 20-80% to extend the battery lifetime [11], [15]. The initial SoC at the arrival time and the desired SoC are normally distributed, $SoC_{i,t_{\text{arr}}} \in U(0.3-05) \times \overline{SoC}_i$, $SoC_i^{\text{Des}} \in U(0.6-0.8) \times \overline{SoC}_i$. A simplified battery degradation based on (3) is used using data from [18]. The average battery degradation cost is then assumed to be 0.032 EUR/kWh. It is also assumed that each household only owns one EV. Therefore, the total number of EVs equals the number of loads.

*3) Price Data:* Capacity remuneration prices data (FCR-N/D) are obtained from Mimer SvK [19]. Energy remuneration prices for FCR-N are the marginal prices of mFRR, also retrieved from Mimer [20]. EV aggregators purchase electricity from the spot market, where prices are obtained from Nord Pool [21]. EV owners who subscribe to the aggregator services will pay charging fees according to the spot prices with a little bit of margin for the EV aggregators (5%); since the charging cost is minimized, they will pay less costs than the uncontrolled charging. EV owners pay near spot prices for charging (added with a 5% aggregator margin) and receive 90% of spot prices for discharging, alongside compensation for battery degradation. The case study applies data from Monday, 20 January 2025, which can be seen in Fig. 8 in Appendix E. The activation rates for FCR-N up and down-regulation are computed from Fingrid frequency data [22]. For the FCR-D, it is more difficult to estimate the activation rates since it only occurs during disturbances. Therefore, activation rates for the FCR-D up and down are randomized with $U(0-0.3)$.

## V. Results and Discussions

### A. Uncontrolled Charging – Baseline

Fig. 2 shows the load profile of the uncontrolled EV charging. The base case scenario shows the overloading of the power grid, which means that grid reinforcement is required if this amount of uncontrolled EV charging occurs. It can be seen that most of the charging is concentrated during the traditional peak hour at night when most residents arrive from work. This is also the time when electricity prices are commonly higher.

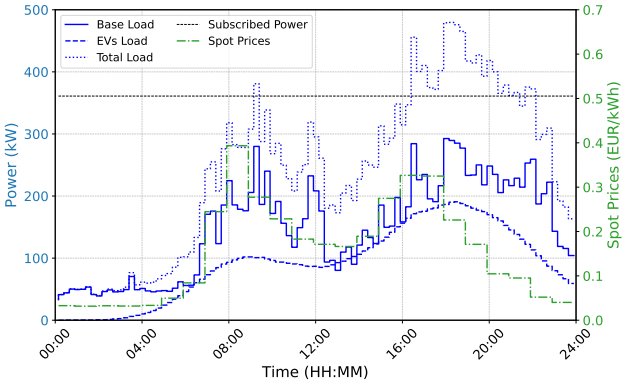


Fig. 2. Uncontrolled EV charging load profile

### B. Smart Charging – Bidirectional

Fig. 3 and 4 show the aggregated load profiles and ancillary service deliveries under the aggregator planning problem. It can be seen in Fig. 3 that using V2G, the additional EV load is spread throughout the day, and there is no grid overloading. The charging/discharging power signals are controlled depending on the availability of the EVs and their accepted bids in the ancillary markets. In reality, the EV aggregators will balance

between planned operations and real-time adjustment after the bids are accepted and activated.

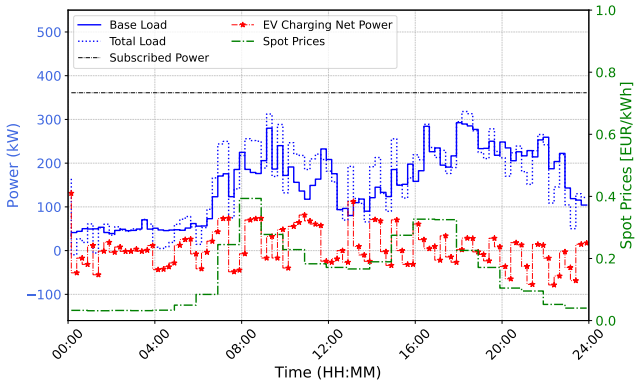


Fig. 3. Bidirectional EV charging load profile

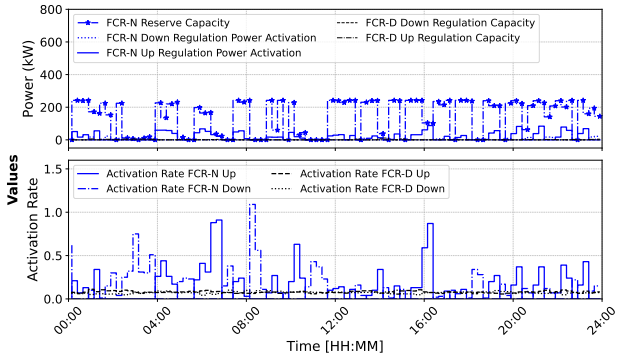


Fig. 4. Ancillary services deliveries

The derived EV charging scheduling is generally feasible. However, infeasible situations may occur where the aggregator cannot deliver the required FCR activation energy. This is particularly possible if the FCR occurs in one direction. Prolonged unidirectional frequency regulation can limit the capability of EVs to provide continuous service as battery SoC constraints become restrictive [23]. An EV aggregator, therefore, needs to maintain the SoC level balance across the EV fleet to ensure sufficient flexibility for the FCR service.

### C. Costs Comparison

The costs for EV owners and aggregators are analyzed to understand the financial feasibility of the business model. The planning model must financially benefit both parties, motivating both to participate in the market. EV owners pay the electricity purchasing costs following the spot prices. In addition, there is also induced cost due to battery degradation when batteries are charged and used. The costs presented in Table I are evaluated from the perspective of EV owners in uncontrolled and bidirectional EV charging. Within the V2G program, EV owners are compensated for battery degradation; consequently, the battery degradation costs incurred by EV owners are 0 EUR. Moreover, the electricity purchase cost is lower and EV owners receive compensation for discharging the EV batteries, making the total cost paid by EV owners significantly lower.

TABLE I
EXPECTED COSTS PAID BY EV OWNERS

| | **Uncontrolled** | **V2G** |
|---|---|---|
| **Costs** | | |
| Electricity purchase [EUR] | 450.7434 | 341.4784 |
| Battery degradation cost [EUR] | 70.3115 | 0.0000 |
| **Incomes** | | |
| Battery degradation compensation [EUR] | 0.0000 | 122.8337 |
| Discharging compensation [EUR] | 0.0000 | 60.1106 |
| **Total cost for EV owners [EUR]** | 519.9717 | 158.5341 |

Besides seeing from the perspective of the EV owners, the EV aggregator participating in the program must also obtain a reasonable profit. Table II shows the revenues and the costs affecting the EV aggregator. In this case study, the FCR-N services have relatively higher compensation than FCR-D. FCR-N participation is the primary profit driver for the EV aggregator; the electricity purchase, discharging compensation, and battery degradation are the key cost factors. The results are sensitive to the different input data, especially the price signals. In this case study, the positive net income of 220.3242 EUR shows that bidirectional smart charging is the financially viable business model for EV aggregators.

TABLE II
EXPECTED REVENUES AND COSTS FOR THE EV AGGREGATOR

| **Cost type** | **V2G [EUR]** |
|---|---|
| **Costs** | |
| FCR-N down energy activation | 4.0997 |
| Discharging compensation | 60.1106 |
| Battery degradation | 125.4965 |
| **Incomes** | |
| FCR-N capacity | 139.2978 |
| FCR-N up energy activation | 270.3261 |
| FCR-D up capacity | 0.0379 |
| FCR-D down capacity | 0.3692 |
| **Total cost for theEV aggregator** | **220.3242** |

## VI. CONCLUSIONS AND FUTURE WORKS

This paper presents a planning model for an EV aggregator participating in ancillary service markets while accounting for uncertainties in mobility patterns, EV types, and ancillary service activations. Monte Carlo simulations of a case study on the Swedish FCR market demonstrate that uncontrolled EV charging can lead to grid overload. In contrast, the proposed bidirectional smart charging strategy efficiently utilizes EV battery flexibility to support grid stability. Simulation results highlight the financial benefits for EV owners and aggregators, reinforcing the proposed model's feasibility and importance. Future work will incorporate price uncertainties and dynamic grid tariffs to improve the model's realism following the real-world market. Moreover, we will extend the model to accommodate multi-market participation to enable EV aggregators to optimize their operations across different ancillary services and incorporate the interaction with retailers in the model.

## REFERENCES

[1] D. Keser and G. Poyrazoglu, "The Impact of Electric Vehicle Charging Stations on Power Distribution Grid by Statistical and Probabilistic

Simulation," in *2020 2nd Global Power, Energy and Communication Conference (GPECOM)*, Oct. 2020, pp. 143–147.
[2] M. Alipour, B. Mohammadi-Ivatloo, M. Moradi-Dalvand, and K. Zare, "Stochastic Scheduling of Aggregators of Plug-In Electric Vehicles for Participation in Energy and Ancillary Service Markets," *Energy*, vol. 118, pp. 1168–1179, Jan. 2017.
[3] M. S. Mastoi, S. Zhuang, H. M. Munir, M. Haris, M. Hassan, M. Usman, S. S. H. Bukhari, and J.-S. Ro, "An in-Depth Analysis of Electric Vehicle Charging Station Infrastructure, Policy Implications, and Future Trends," *Energy Reports*, vol. 8, pp. 11 504–11 529, Nov. 2022.
[4] A. Aldik, A. T. Al-Awami, E. Sortomme, A. M. Muqbel, and M. Shahidehpour, "A Planning Model for Electric Vehicle Aggregators Providing Ancillary Services," *IEEE Access*, vol. 6, pp. 70 685–70 697, 2018.
[5] H. Ren, A. Zhang, F. Wang, X. Yan, Y. Li, N. Duić, M. Shafie-khah, and J. P. S. Catalão, "Optimal Scheduling of an EV Aggregator for Demand Response Considering Triple Level Benefits of Three-Parties," *International Journal of Electrical Power & Energy Systems*, vol. 125, p. 106447, Feb. 2021.
[6] C. Sandels, U. Franke, N. Ingvar, L. Nordström, and R. Hamrén, "Vehicle to Grid — Monte Carlo Simulations for Optimal Aggregator Strategies," in *2010 International Conference on Power System Technology*, Oct. 2010, pp. 1–8.
[7] Svenska Kraftnät, "Information on Different Ancillary Services," Oct. 2023. [Online]. Available: https://www.svk.se/en/stakeholders-portal/electricity-market/provision-of-ancillary-services/information-on-different-ancillary-services/
[8] A. Thingvad, C. Ziras, G. L. Ray, J. Engelhardt, R. R. Mosbæk, and M. Marinelli, "Economic Value of Multi-Market Bidding in Nordic Frequency Markets," in *2022 International Conference on Renewable Energies and Smart Technologies (REST)*, vol. I, Jul. 2022, pp. 1–5.
[9] Svenska Kraftnät, "Om Olika Reserver (About Different Reserves)," Jan. 2025. [Online]. Available: https://www.svk.se/aktorsportalen/bidra-med-reserver/om-olika-reserver/
[10] European Network of Transmission System Operators for Electricity, "Technical Requirements for Frequency Containment Reserve Provision in the Nordic Synchronous Area." [Online]. Available: https://www.svk.se/siteassets/aktorsportalen/bidra-med-reserver/om-olika-reserver/fcr/fcr-technical-requirements-may-23.pdf
[11] E. D. Kostopoulos, G. C. Spyropoulos, and J. K. Kaldellis, "Real-World Study for the Optimal Charging of Electric Vehicles," *Energy Reports*, vol. 6, pp. 418–426, Nov. 2020.
[12] K. P. Schneider, B. A. Mather, B. C. Pal, C.-W. Ten, G. J. Shirek, H. Zhu, J. C. Fuller, J. L. R. Pereira, L. F. Ochoa, L. R. de Araujo, R. C. Dugan, S. Matthias, S. Paudyal, T. E. McDermott, and W. Kersting, "Analytic Considerations and Design Basis for the IEEE Distribution Test Feeders," *IEEE Transactions on Power Systems*, vol. 33, no. 3, pp. 3181–3188, May 2018.
[13] M. H. Wahlström and B. Hårsman, "Residential Energy Consumption and Conservation," *Energy and Buildings*, vol. 102, pp. 58–66, Sep. 2015.
[14] Swedish Institute for Transport and Communications Analysis, "RES 2005-2006 The National Travel Survey," Swedish Institute for Transport and Communications Analysis, Sweden, Tech. Rep., 2007. [Online]. Available: https://www.trafa.se/globalassets/sika/sika-statistik/ss_2007_19_eng.pdf
[15] D. Anggraini, M. Amelin, and L. Söder, "Electric Vehicle Charging Considering Grid Limitation in Residential Areas," in *2024 IEEE Transportation Electrification Conference and Expo (ITEC)*, Jun. 2024, pp. 1–6.
[16] European Comission, "European EV Market Analysis: Strong Growth Continues as Plug-in Vehicle Registrations Rise in April." [Online]. Available: https://alternative-fuels-observatory.ec.europa.eu/general-information/news/european-ev-market-analysis-strong-growth-continues-plug-vehicle
[17] Y. Iwafune and T. Kawai, "Data Analysis and Estimation of the Conversion Efficiency of Bidirectional EV Chargers Using Home Energy Management Systems Data," *Smart Energy*, vol. 15, p. 100145, Aug. 2024.
[18] S. Ayyadi, H. Bilil, and M. Maaroufi, "Optimal Charging of Electric Vehicles in Residential Area," *Sustainable Energy, Grids and Networks*, vol. 19, p. 100240, Sep. 2019.
[19] Svenska Kraftnät, "Mimer | FCR." [Online]. Available: https://mimer.svk.se/PrimaryRegulation/PrimaryRegulationIndex
[20] ——, "Mimer | Manuell frekvensåterställningsreserv," 2025. [Online]. Available: mimer.svk.se/ManualFrequencyRestorationReserve
[21] Nord Pool, "Day-Ahead Prices," Jan. 2025. [Online]. Available: data.nordpoolgroup.com
[22] FINGRID, "FINGRID Datasets." [Online]. Available: https://data.fingrid.fi/en/data?datasets=177
[23] P. Codani, Y. Perez, and M. Petit, "Financial Shortfall for Electric Vehicles: Economic Impacts of Transmission System Operators Market Designs," *Energy*, vol. 113, pp. 422–431, Oct. 2016.
[24] E. Gómez-Déniz, J. M. Sarabia, and E. Calderín-Ojeda, "Bimodal normal distribution: Extensions and applications," *Journal of Computational and Applied Mathematics*, vol. 388, p. 113292, May 2021.
[25] V. Smirnov, Z. Ma, and D. Volchenkov, "Invited article by M. Gidea Extreme events and emergency scales," *Communications in Nonlinear Science and Numerical Simulation*, vol. 90, p. 105350, Nov. 2020.

## APPENDIX A
## SWEDISH ANCILLARY SERVICE MARKETS

There are three main categories of ancillary services in the Swedish system, which are the remedial action, FCR, and Fast Frequency Reserve (FFR). The overview of all services is available in [7]. Since FCR is already discussed in Section II; this appendix section will give an overview of the other products listed in Fig. 1. FFR, or remedial action, is an automatically activated product for changes in frequency under a low inertia level. It is an upward regulation with 30 seconds of endurance and is ready for activation within 15 minutes. The minimum bid size for this is 0.5 MW. Frequency restoration Reserves (FRR) contains automatic Frequency Restoration Reserve (aFRR) and manual Frequency Restoration Reserve (mFRR). aFRR is automatically activated to handle frequency deviations from 50 Hz. mFRR is manually activated when SvK requested it. The activation time for both are 5 and 15 minutes, respectively. Both have upward/downward regulation with a 1 MW minimum bid size.

## APPENDIX B
## MONTE CARLO SIMULATIONS

$K$ number of scenarios are simulated for the two charging schemes. The PDFs of the uncertain inputs will be used to generate random numbers. After obtaining independent observations $x_1, \ldots, x_k$ from a random variable $X$ with an expectation value E[X], the unbiased estimation of E[X] is computed as:

$$m_X = \frac{1}{k} \sum_{s=1}^{k} x_s. \tag{7}$$

## APPENDIX C
## DISTRIBUTION NETWORK TEST SYSTEM

The topology of the modified IEEE European Low Voltage Test Feeder is shown in Fig. 5. It has a radial topology with no close loops in the network. The aggregated load profile is scaled from the time series simulations provided by the system.

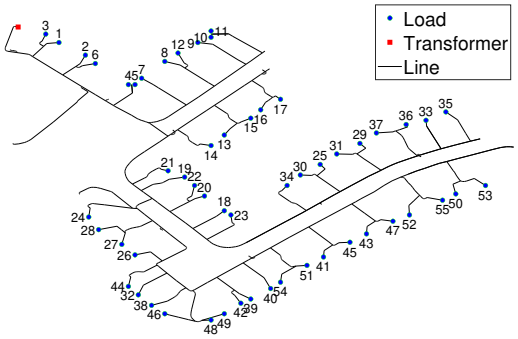


Fig. 5. IEEE European LV test feeder [12]

## APPENDIX D
## MOBILITY PATTERNS

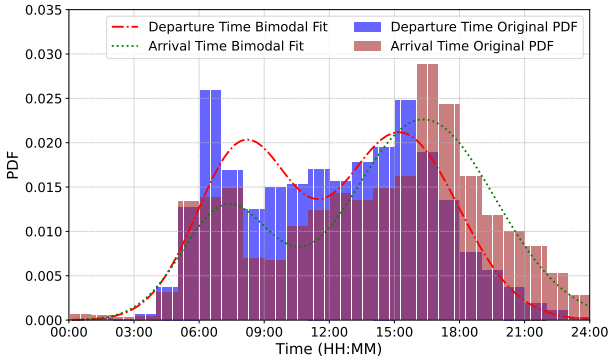


Fig. 6. PDFs of the departure and arrival time

Two PDFs are selected to represent the mobility patterns data used in the case study: bimodal distribution and extreme value distribution. The bimodal distribution occurs naturally in different scenarios. This distribution can be represented as a combination of two normal distributions [24].

$$f_{bim}(w) = p\frac{1}{\sigma_1\sqrt{2\pi}}\exp\left(-\frac{(w-\mu_1)^2}{2\sigma_1^2}\right) + (1-p)\frac{1}{\sigma_2\sqrt{2\pi}}\exp\left(-\frac{(w-\mu_2)^2}{2\sigma_2^2}\right) \tag{8}$$

$\mu_1$ and $\mu_2$ are the mean values of the two normal distributions. $\sigma_1$ and $\sigma_2$ denote the standard deviations of the two normal distributions. $p$ is the weighing factor that represents the relative contribution of the first normal distribution to the whole bimodal distribution. The bimodal distribution is used to fit the departure and arrival time PDFs, such as given in Fig. 6.

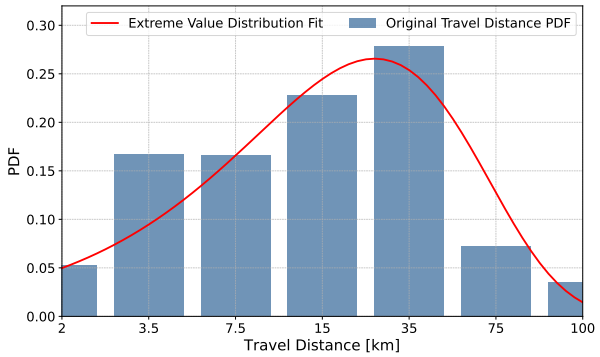


Fig. 7. PDF of the travel distance

The PDF of an extreme value distribution with location parameter $\zeta$ and scale parameter $\rho$ is given below [25]:

$$f_{ext}(w) = \frac{1}{\rho}\exp\left(-\left(\frac{w-\zeta}{\rho}\right)\right) - \exp\left(-\frac{w-\zeta}{\rho}\right) \tag{9}$$

Extreme value distribution is used to model the travel distance data, which is shown in Fig. 7.

## APPENDIX E
## PRICE DATA

Fig. 8 shows the time series prices of electricity and ancillary services used in the simulation. The data is taken for Monday, 20 January 2025. The explanation for each data is provided in section IV-C3.

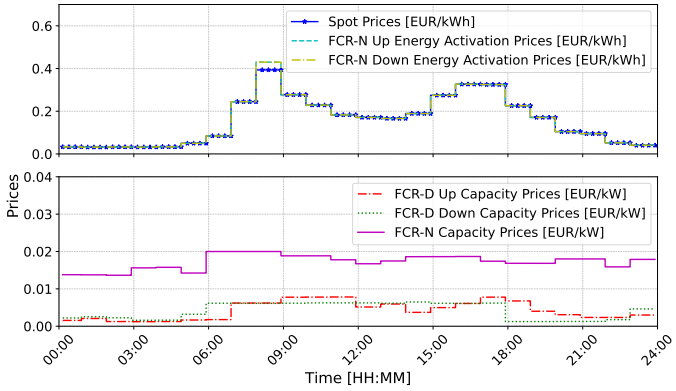


Fig. 8. Price data

## APPENDIX F
## EV SPECIFICATIONS

Table III shows four EV types used in the case study, including their battery capacities and the percentage of market shares.

TABLE III
EV SPECIFICATIONS [15]

| Type | Model | Market share [%] | $\overline{E}_i$ [kWh] |
|---|---|---|---|
| 1 | Tesla Model Y | 39.30 | 57.5 |
| 2 | Volkswagen ID.4 Pro Performance | 24.37 | 77 |
| 3 | Volvo XC40 Recharge Single Motor ER | 14.72 | 79 |
| 4 | Volkswagen ID.3 Pro | 21.61 | 58 |